Optimal Planning of Hybrid AC/DC Low-voltage Distribution Networks Considering DC Conversion of Three-phase Four-wire Low-voltage AC Systems

Bo Zhang, Lu Zhang, Wei Tang, Gen Li, and Chen Wang

***Abstract*—The increasing integration of distributed household photovoltaics (PVs) and electric vehicles (EVs) may further aggravate voltage violations and unbalance of low-voltage distribution networks (LVDNs). DC distribution networks can increase the accommodation of PVs and EVs and mitigate mutilple power quality problems by the flexible power regulation capability of voltage source converters. This paper proposes schemes to establish hybrid AC/DC LVDNs considering the conversion of the existing three-phase four-wire low-voltage AC systems to DC operation. The characteristics and DC conversion constraints of typical LVDNs are analyzed. In addition, converter configurations for typical LVDNs are proposed based on the three-phase four-wire characteristics and quantitative analysis of various DC configurations. Moreover, an optimal planning method of hybrid AC/DC LVDNs is proposed, which is modeled as a bi-level programming model considering the annual investments and three-phase unbalance. Simulations are conducted to verify the effectiveness of the proposed optimal planning method. Simulation results show that the proposed optimal planning method can increase the integration of PVs while simultaneously reducing issues related to voltage violation and unbalance.**

***Index Terms*—Optimal planning, low-voltage distribution network, three-phase unbalance, DC conversion.**

NOMENCLATURE

A. Parameters

Φ_i	Upstream node set of node i
Ψ_i	Downstream node set of node i
ϕ	Phase difference between voltage and current
λ	Fixed average annual cost coefficient
φ	Three phases
C_{VSC}	Investment cost per apparent power of voltage source converter (VSC)
$I_{AC}^{\max}$, $I_{DC}^{\max}$	The maximum currents of AC and DC lines
L	Service life of VSC
L_{VSC}	Candidate location set of VSCs
N_{AC}, N_{DC}	Node sets of AC and DC low-voltage distribution networks (LVDNs)
$P_{\max}^{AC}$, $P_{\max}^{DC}$	The maximum transfer capacities of AC and DC LVDNs
r	Discount rate
r_{AC}, r_{DC}	Resistances of AC and DC lines
R_{ji}^{φ}	Resistance of phase φ of AC branch ji
R_{ji}	Resistance of DC branch ji
$S_{VSC}^{\max}$	The maximum allowable installed capacity of VSC
$S_{\max}^{AC}$	The maximum apparent power capacity of AC lines
T	Number of scheduling periods in a day
U_{AC}^{rated}, U_{DC}^{rated}	Rated voltages of AC and DC LVDNs
$U_{\min}$, $U_{\max}$	The minimum and maximum allowable voltages
X_{ji}^{φ}	Reactance of phase φ of AC branch ji
$\boldsymbol{Z}_{AC}$	Line impedance matrix of AC lines

B. Variables

ε	Convergence error
$\Delta \boldsymbol{U}_{AC}$	Voltage drop in AC network
ΔU_{DC}	Voltage drop in DC network
C_{invest}	Annual investment of installed VSCs
F_{UL}, F_{LL}	Objective functions of upper and lower models
F_{K_U}, F_{K_U-1}	Upper-level objective function values for K_U and K_U-1 iterations
I_{VUF}	Three-phase voltage unbalanced factor (VUF)

Manuscript received: July 7, 2022; revised: October 19, 2022; accepted: June 24, 2023. Date of CrossCheck: June 24, 2023. Date of online publication: July 26, 2023.

This work was supported by the National Key Research and Development Program of China (No. 2019YFE0118400).

B. Zhang, L. Zhang, and W. Tang (corresponding author) are with the College of Information and Electrical Engineering, China Agricultural University, Beijing 100083, China (e-mail: zhangbo1223@foxmail.com; zhanglu1@cau.edu.cn; wei_tang@cau.edu.cn).

G. Li is with the Electric Energy Group, Department of Engineering Technology, Technical University of Denmark (DTU), 2750 Ballerup, Denmark (e-mail: genli@dtu.dk).

C. Wang is with the Power Distribution Technology Center, State Grid Beijing Electric Power Research Institute, Beijing 100075, China (e-mail: chen_wang2022@126.com).

DOI: 10.35833/MPCE.2022.000404

$I_{VUF,i}$	VUF of node i
$\boldsymbol{I}_{in}$	Current vector
$\boldsymbol{I}_{in,\varphi}$, $\boldsymbol{I}_{in,n}$	Current vectors of phase wires and neutral wires
I_{ji}^{φ}	Current of phase φ of AC branch ji
I_{ji}	Current of DC branch ji
$I_{VUF,\ i}$	VUF of node i
K_U	Number of iterations of upper optimization
$K_U^{\max}$	The maximum iterations of upper optimization
L_{VSC}^{n}	Connection locations of the n^{th} VSC
N_{AC}	Node set of AC LVDN
N_{VSC}	Number of installed VSCs
P_{VSC}^{AC}, P_{VSC}^{DC}	Active power outputs of VSC injected to AC and DC networks
P_{VSC}^{loss}, P_{VSC}^{rated}	Power loss and rated power of VSC
P_{ji}, P_{ik}	Line power of DC branches ji and ik
P_i	Injected power of node i in DC LVDN
P_{ji}^{φ}, P_{ik}^{φ}	Active power of AC branches ji and ik
P_i^{φ}, Q_i^{φ}	Injected power of node i in AC LVDN
Q_{ji}^{φ}, Q_{ik}^{φ}	Reactive power of AC branches ji and ik
Q_{VSC}^{AC}	Reactive power of VSC injected to AC system
S_{ji}^{AC}	Line apparent power of AC branch ji
S_{VSC}^{n}	Installed capacity of the n^{th} VSC
U_i	Voltage of node i in DC network
U_i^{avr}, U_i^{φ}	Three-phase average voltage and phase φ voltage of node i in AC LVDN
$V_{\max}$, $V_{\min}$	Allowable maximum and minimum voltages in LVDN
V_i^{avr}	Three-phase average voltage of node i

I. Introduction

LOW-VOLTAGE distribution networks (LVDNs) are required to achieve a high power quality standard to maintain the reliable power supply of end-users. However, the three-phase unbalanced issues caused by unbalanced loads and parameters of LVDNs may exacerbate the voltage quality and increase power losses [1]. The increasing integration of distributed household photovoltaics (PVs) and electric vehicle (EV) chargers may further aggravate the unbalance as numbers of PVs and EV chargers are connected in single-phase mode [2], [3]. The installation of distributed generations (DGs) and loads may lead to overload problems of low-voltage (LV) lines and distribution transformers (DTs). Meanwhile, voltage profile may be affected by the intermittence of DG outputs and loads due to the limited power transfer capacity and flexible control capability of AC LVDNs [4]. Therefore, the power quality issues of LVDNs including overloads, unbalanced issues, and voltage violations, have to be addressed.

The above problems can be relieved by building new distribution lines and transformers. However, the solution is considered as costly and infeasible as the unbalance may still exist and the land space in urban areas is limited [5]. Some power electronic devices can improve the node voltages by flexible reactive power regulation such as static var generators (SVGs). However, the voltages in AC LVDNs are coupled with active and reactive power due to the large ratio of resistance and reactance [6]. The performance of these reactive power compensation devices is hence limited in LVDNs. Flexible power flow control between LV lines and three phases presents a potential solution to addressing the power quality problems. However, AC distribution networks are normally radial. Phase-change switches (PCSs) can change the connected phase of the residential customer to mitigate the unbalance [7], [8]. However, PCSs are mainly installed in places with three-phase commutation and the switch operation may cause voltage sags [9].

The DC distribution network can effectively address the uncertainties from PVs and EVs [10], due to its advantages of flexible power control capability and high power transfer capacity [11], [12]. Flexible interconnection between AC and DC lines also enables the controllable power flow [13]. Moreover, the three-phase power can be regulated separately through voltage source converters (VSCs) [14], [15] which are considered as the interface of the hybrid AC/DC distribution networks. Hybrid AC/DC LVDNs offer an alternative method to overcome the limitations of AC LVDNs and enable flexible power control between LV lines and three phases.

One viable techno-economic solution to implementing a DC distribution network is to convert the operation mode of existing AC systems into DC [16]. Existing applications of hybrid AC/DC technologies are mainly focused on high-voltage transmission systems [17], [18], medium-voltage distribution networks (MVDNs) [19], [20], and new-built LV DC microgrids [21]. Reference [22] presents a DC conversion method for MVDNs and proposes the corresponding optimal operation methods including day-ahead scheduling and real-time control. Reference [23] presents a comprehensive planning method for hybrid AC/DC MVDNs and LVDNs, which shows that hybrid AC/DC systems reduce costs in the presence of high penetration of DGs. A planning method for hybrid AC/DC transmission and distribution systems is proposed, which aims to address the challenges associated with multidimensional and nonlinear system configuration [24]. Reference [25] shows that the reconfigurable parallel AC-DC links can serve as an efficient and economical choice, particularly for delivering high power at medium-voltage (MV) level to short distances. A systematic reconfiguration strategy employing a flexible DC link is proposed in [26], aiming to ensure the high power transfer capacity during $n-1$ contingency events. Reference [27] proposes an optimal planning method of hybrid AC/DC MVDNs, in which the DC conversion of existing AC lines is considered to achieve the minimum cost and the maximum renewable energy integration. However, the research only investigates the DC conversion from the three-phase AC MVDNs. The optimal DC conversion of three-phase four-wire AC LVDNs is not investigated.

Although there have been applications of hybrid AC/DC distribution networks, the DC conversion of LVDNs is still under study. Shortcomings of the existing DC conversion

and planning solutions of LVDNs include:

1) The existing conversion methods rarely consider the widely used three-phase four-wire configuration in LVDNs. In addition, there are no quantitative evaluation methods for the improvement of DC upgrading on power supply capacities and voltage drops. The capacity of the existing LV wires is not fully utilized by the existing methods which focus on three-phase three-wire MVDNs.

2) The optimal planning of hybrid AC/DC LVDNs considering investments and comprehensive improvement of multiple power quality issues including three-phase unbalance and voltage violations, is still being studied. Moreover, a 24-hour optimal dispatch considering the coordination among multiple lines and phases in LVDNs needs to be achieved to calculate the benefits. However, the planning of DC distribution networks mainly focuses on MVDN, and the improvement of the unbalanced issues is not considered. Although the existing planning methods for AC LVDNs take the unbalance into account, the three-phase regulation of VSCs is still not considered.

This paper aims to convert parts of the three-phase four-wire AC lines into DC operation, thereby establishing hybrid AC/DC LVDNs to increase the power capacity and operation performance. An optimal planning method of hybrid AC/DC LVDNs is proposed, considering the DC conversion's configuration, costs, and capability of mitigating the three-phase unbalanced degree. The main contributions of this paper are summarized as follows.

1) The characteristics and DC conversion constraints of typical LVDNs are analyzed. The converter configuration and DC connection mode for LVDNs are proposed considering the three-phase four-wire characteristics and quantitative analysis of various DC configurations.

2) An optimal planning method of hybrid AC/DC LVDNs converted from AC LVDNs is proposed considering three-phase power dispatch of VSCs, in which a bi-level model is built to minimize the three-phase unbalance and capital costs.

The rest of paper is organized as follows. Section II presents the problem statement. Section III analyzes converter configuration and connection mode for three-phase four-wire LVDNs. Section IV proposes the optimal planning method of hybrid AC/DC LVDNs. Section V presents the simulation and result analysis. Section VI concludes this paper.

II. Problem Statement

An LVDN with two DTs (DT1 and DT2) and five LV lines (L1-L5) is shown in Fig. 1(a). High-penetration distributed PVs and EV charging points are integrated into the LVDN. A, B and C represent connected phases of PVs and EV charging points in Fig. 1(a). The following assumptions have been made in this paper: the AC LV lines are in three-phase four-wire configuration; load level and PV capacities in the LVDN increase year by year; DC charging points and PV generations can be relocated to adjacent DC lines after the DC conversion; and the rated DC voltage of the LVDN is ±375 V.

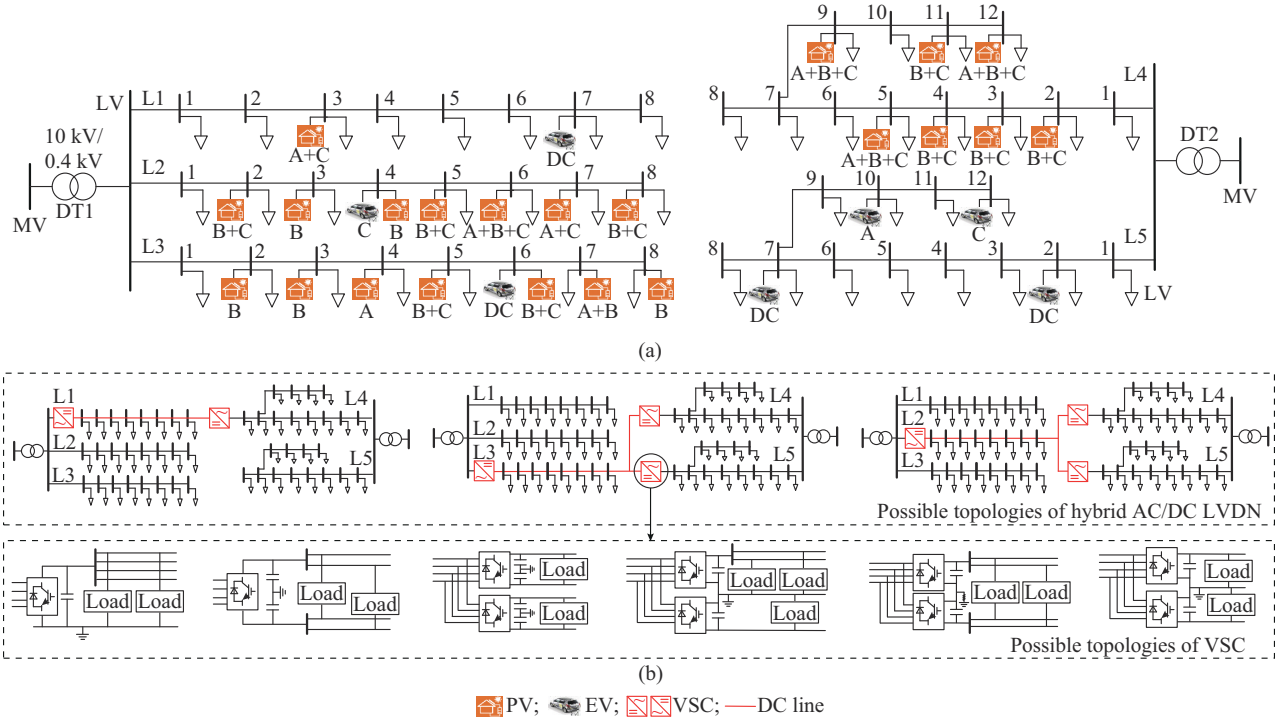

Fig. 1. Hybrid AC/DC LVDN considering DC conversion. (a) Five-feeder LVDN. (b) Possible topologies of hybrid AC/DC LVDN and VSC.

In this paper, two distribution areas are interconnected with DC links considering the DC conversion of the LV AC lines. The DC conversion will enhance the power capacities and realize comprehensive improvement of power quality in LVDNs using the flexible control capability of VSCs. An optimal planning method of the hybrid AC/DC LVDN is therefore needed and proposed in this paper. Figure 1(b) shows some possible topologies of hybrid AC/DC LVDN and VSC.

The problem to be solved in this paper is to propose an optimal planning method for hybrid AC/DC LVDNs to select the optimal topology and converter configuration among various possible configurations. Therefore, the proposed optimal planning method consists of two parts: selection of the DC converter configurations and topology optimization of hybrid AC/DC LVDNs.

III. Converter Configuration and Connection Mode for Three-phase Four-wire LVDNs

A. Characteristics and Constraints of Typical LVDNs

LVDNs are typically with a three-phase four-wire configuration, distinguishing them from MVDNs that utilize a three-phase three-wire configuration. The characteristics of three typical LVDNs in urban, town, and rural areas are analyzed. Figure 2 shows the network structures and sectional views of the wires for the three typical LVDNs, where N denotes neutral wire.

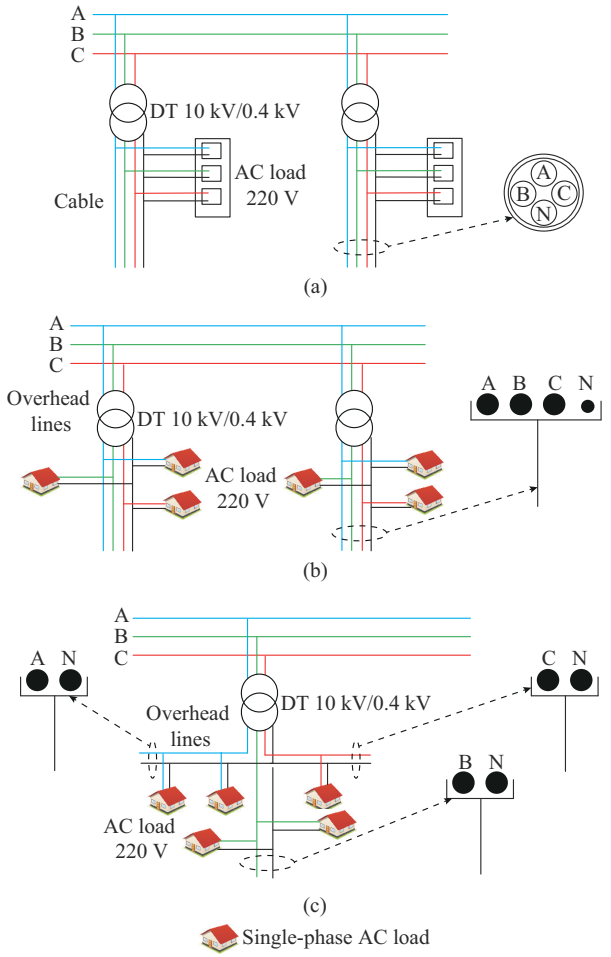

Fig. 2. Network structures and sectional views of wires for three typical LVDNs. (a) Urban areas. (b) Town areas. (c) Rural areas.

In urban LVDNs, the utilization of four-core cables is prevalent due to the limited corridor space, as shown in Fig. 2(a). Generally, the material and diameter of the four cores are the same [28], and the current-carrying capacities of the neutral wire and the phase wires of the cables are the same. The rapid growth of loads in urban LVDNs may lead to the overload of DTs and lines. The increasing integration of DC loads such as EVs may further aggravate multiple power quality issues. Therefore, DC conversion schemes for urban LVDNs need to meet the requirements of high power quality and the increasing load demands.

Town LVDNs, as shown in Fig. 2(b), usually use three-phase four-wire overhead lines, of which the neutral wire is a bare copper conductor and is thinner than other phase wires. The increasing integration of household PVs may cause voltage violations and fluctuations. Therefore, improving PV accommodation is an urgent issue in town LVDNs. The neutral wires of the overhead lines cannot be used to transmit power in DC systems because the current carrying capacity of the neutral wire is smaller than other phase wires.

In some rural areas, the three-phase lines of LVDNs supply power separately. This structure is split into three circuits from the terminal of the DT for single-phase power supply, as shown in Fig. 2(c), which may cause serious three-phase unbalance problems. In this structure, the current carrying capacities of the neutral wire and other phase wires are the same after splitting. DC conversion scheme for this kind of structure needs to ensure that there are three circuits.

B. Converter Configuration Method for LVDNs

1) Quantitative Analysis of DC Configurations Converted from AC LVDNs

The common VSC configurations include asymmetric monopole, symmetric monopole, and bipolar configurations [22]. The possible DC configurations converted from AC LVDNs are proposed, as shown in Fig. 3, and quantitative analyzed, based on these common configurations and the three-phase four-wire characteristics of LVDNs.

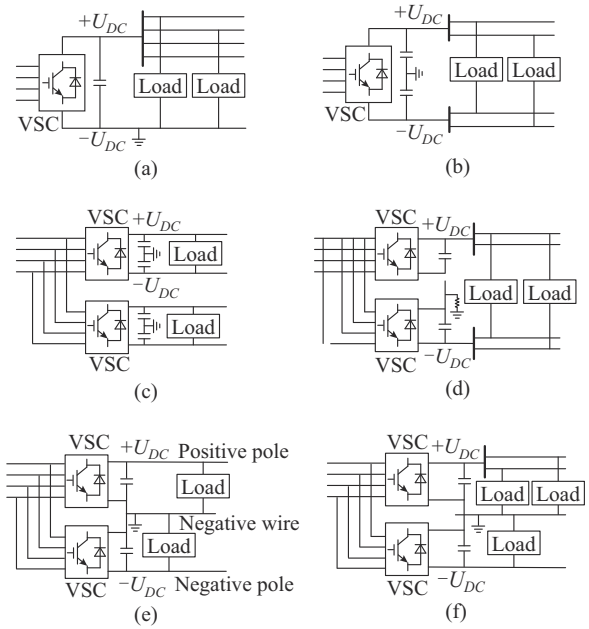

Fig. 3. Possible DC configurations converted from AC LVDNs. (a) Asymmetric monopole configuration. (b) Symmetric monopole configuration. (c) Parallel operation monopole configuration. (d) Bipolar configuration. (e) Bipolar configuration with a dedicated metallic return. (f) Improved bipolar configuration.

By converting the AC LVDN into an asymmetric monopole configuration, the original four wires can be combined as the positive pole, as illustrated in Fig. 3(a). An additional conductor is required as the neutral wire, which must be capable of carrying the full load current but requires low insulation requirement and cost due to its zero voltage potential to the ground. The load can be connected between any DC conductor and the neutral wire.

As shown in Fig. 3(b), the original four wires can be fully utilized to establish a symmetric monopole configuration, with two wires serving as the positive pole and the remaining two as the negative pole. The load can be connected between any positive and negative poles. This conversion does not need new conductors.

Figure 3(c) illustrates the parallel operation monopoles utilizing two VSCs along with the existing four AC wires. Compared with the symmetric monopole configuration, this configuration offers enhanced reliability as any failure in one DC circuit has no impact on the other circuit. This configuration does not require the additional new wires, but two VSCs with half of the maximum capacity of the original LVDNs are required.

As shown in Fig. 3(d), the positive and negative poles of the bipolar configuration utilize two wires, repectively. The load can be connected between any positive and negative wires. This structure does not need a neutral wire. This rigid bipolar system with high-impedance DC grounding will be shut down if one pole fails. Therefore, the reliability is lower than the bipolar system with a dedicated metallic return, which is shown in Fig. 3(e).

The bipolar configuration employs three of the original AC wires, serving as the positive pole, negative pole, and neutral wire, respectively, as illustrated in Fig. 3(e). If the load currents in the positive and negative poles are balanced, there will be no current in the neutral wire. Failures in one pole will not affect the operation of the other pole. In this conversion, the rest wire can be used as a spare conductor.

To make full use of the four existing wires, the configuration shown in Fig. 3(f) can be obtained by adding the rest wire in either the positive pole or the negative pole. In this configuration, the load current difference between the positive and negative poles cannot exceed the maximum current capacity of the neutral wire. For example, if all loads are connected to the two wires in the positive pole and the positive pole is fully loaded, then the neutral wire may be overloaded due to the unbalanced current in it. Two VSCs with a capacity of half the maximum capacity of the original LVDNs are required in this configuration.

After being converted into DC operation, the power transfer capacities and voltage drops of various DC configurations have changed in comparison to the original LVDNs, which can be calculated as follows.

According to [22], the resistance relationship before and after the conversion is:

$$\begin{cases} r_{DC} = 0.98 r_{AC} \\ I_{DC}^{\max} = 1.01 I_{AC}^{\max} \end{cases} \tag{1}$$

The maximum power transfer capacity of the AC LVDN is the maximum power under the three-phase balanced condition.

$$P_{\max}^{AC} = \sqrt{3}\, U_{AC}^{rated} I_{AC}^{\max} \cos\phi \tag{2}$$

$P_{\max}^{DC}$ for the configurations of Fig. 3(a)-(d) is:

$$P_{\max}^{DC} = 4 U_{DC}^{rated} I_{DC}^{\max} \tag{3}$$

$P_{\max}^{DC}$ for the configuration of Fig. 3(e) is:

$$P_{\max}^{DC} = 2 U_{DC}^{rated} I_{DC}^{\max} \tag{4}$$

$P_{\max}^{DC}$ for the configuration of Fig. 3(f) is:

$$P_{\max}^{DC} = 3 U_{DC}^{rated} I_{DC}^{\max} \tag{5}$$

The voltage drop of the three-phase four-wire LVDNs, for the given load power P_L and Q_L, can be expressed as:

$$\Delta \boldsymbol{U}_{AC} = \boldsymbol{Z}_{AC} \boldsymbol{I}_{in} \tag{6}$$

$$\begin{cases} \boldsymbol{I}_{in,\varphi} = (P_{L,\varphi} - \mathrm{j} Q_{L,\varphi}) / U_{AC,\varphi}^{rated} \quad \varphi \in \{a, b, c\} \\ \boldsymbol{I}_{in,n} = -(\boldsymbol{I}_{in,a} + \boldsymbol{I}_{in,b} + \boldsymbol{I}_{in,c}) \end{cases} \tag{7}$$

Assuming that the active load P_L is evenly distributed on each DC line after the conversion. For the configurations of Fig. 3(a)-(d), the voltage drop in DC network can be calculated as:

$$\Delta U_{DC} = \frac{P_L}{4 U_{DC}^{rated}} r_{DC} \tag{8}$$

For the configuration of Fig. 3(e), the DC voltage drop is:

$$\Delta U_{DC} = \frac{P_L}{2 U_{DC}^{rated}} r_{DC} \tag{9}$$

For the configuration of Fig. 3(f), the DC voltage drop is:

$$\Delta U_{DC} = \frac{P_L}{3 U_{DC}^{rated}} r_{DC} \tag{10}$$

2) Converter Configuration and Connection Mode for LVDNs

Considering the characteristics and DC conversion constraints of typical LVDNs as well as quantitative analysis of various DC configurations, the converter configuration and DC connection mode for LVDNs are proposed in this part. The network structures for LVDNs after DC conversion are shown in Fig. 4.

For urban LVDNs, high power transfer capacity and reliability are required to meet the growing load demands. A favorable method is to utilize the original four wires of the four-core cables, which have the same current-carrying capacities, as the positive and negative poles. Therefore, the parallel operation monopole configuration can be adopted in urban areas. In this configuration, any two of the original four wires are utilized as the negative pole, while the remaining two are utilized as the positive pole, as shown in Fig. 4(a). After converting AC lines into DC operation, DC loads such as EVs can be relocated to the adjacent DC lines. The transfer capacity and voltage drop of this configuration can be calculated by (3) and (8), respectively.

For town LVDNs, only three-phase wires of the overhead lines can be used to transmit DC power because the current carrying capacity of the neutral wire is smaller than that of other wires. Therefore, the bipolar configuration with a dedicated metallic return shown in Fig. 3(e) can be adopted. The

AC and DC distribution lines can be interconnected by converters after DC conversion, as shown in Fig. 4(b). The transfer capacity and voltage drop of this configuration can be calculated by (4) and (9), respectively.

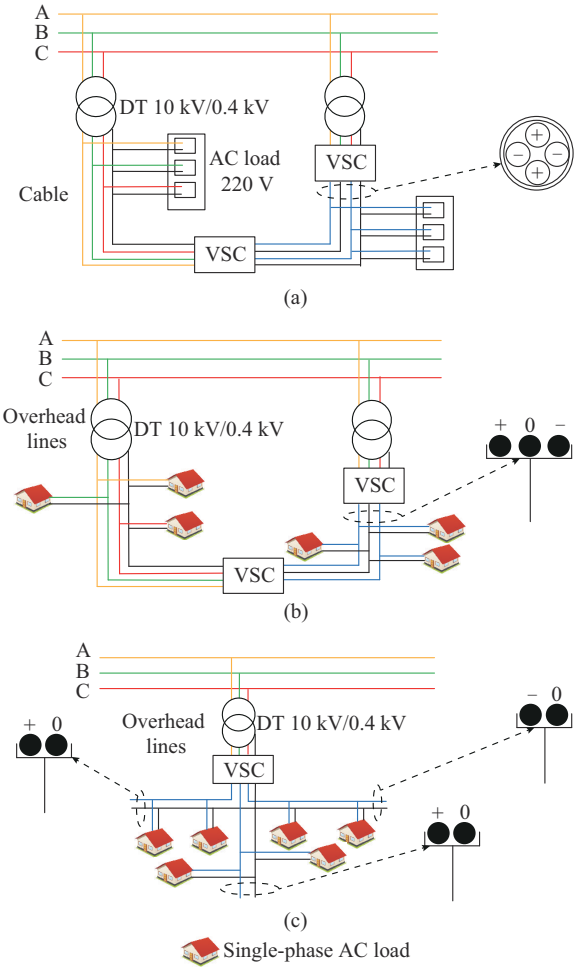

Fig. 4. Network structures for LVDNs after DC conversion. (a) Urban areas. (b) Town areas. (c) Rural areas.

For rural LVDNs in single-phase power supply mode, the DC conversion scheme needs to ensure that there are three circuits. Therefore, the improved bipolar configuration with a dedicated metallic return, as shown in Fig. 3(f), is adopted for rural LVDNs, which can make full use of the existing AC lines, as shown in Fig. 4(c). The transfer capacity and voltage drop of this configuration can be calculated by (5) and (10), respectively.

The proposed converter configurations for three typical LVDNs consider the three-phase four-wire characteristics and quantitative analysis of various DC configurations, which can fully utilize the capacity of the existing LV wires.

IV. Optimal Configuration for Hybrid AC/DC LVDNs

Before the optimization process of the hybrid AC/DC LVDN, one of the three typical DC conversion structures can be selected according to the characteristics of the LVDN. Then, the topology of hybrid AC/DC LVDNs are optimized by the proposed optimal planning method. The proposed optimal planning method is formulated as a bi-level programming model. The VSC capacity and topologies of the hybrid AC/DC LVDNs are optimized at the upper level. Then, at the lower level, a 24-hour optimal dispatching is achieved considering the load level, power flow constraint, and VSC capacity constraints. The results of the lower level, including the three-phase power of the VSCs for 24 hours and three-phase unbalanced degree, will be returned to the upper level to update the overall objectives and generate a better configuration result for the hybrid AC/DC LVDNs. The optimal configuration results are finally obtained through iterations between the two levels.

Notice that the proposed optimal planning method includes three types of VSCs, i.e., VSCs at the terminal of the DC line (the VSC1 in Fig. 5), VSCs for interconnection of the lines (the VSC2 in Fig. 5), and VSCs for connecting loads and DGs (the VSC3 in Fig. 5). The capacities of VSCs at the terminal of the DC line are determined by the capacities of the line and transformer. The capacities of VSCs for connecting loads and DGs are determined by the maximum loads and DG power. Only the capacities of VSCs for interconnection of the lines are optimized by the proposed optimal planning method.

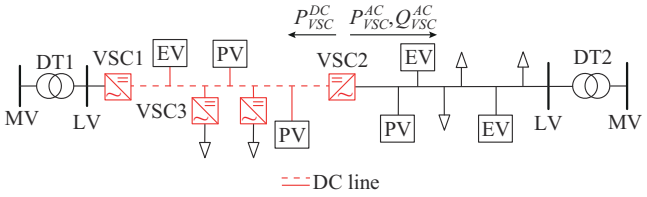

Fig. 5. Hybrid AC/DC LVDN.

The topologies of the hybrid AC/DC LVDNs can be achieved by installing VSCs and selecting the reasonable VSC control modes. In Fig. 5, VSC1 operates in the V_{dc}-Q control mode to establish and regulate the DC-side voltage, while VSC2 operates in the P-Q control mode to regulate the transfer power. The unbalanced degree of the AC LVDNs can be alleviated by independently controlling the three-phase power output of the VSC2, which is optimized in the lower-level model.

A. Upper-level Optimization Model

The upper-level optimization model is established with the objective function of minimizing annual investments and three-phase unbalanced degree of the hybrid AC/DC LVDNs, as shown in (11), which is also the overall objective function of the optimization model. The installed capacities and locations of the VSCs are optimized at the upper level, which determines the topology of hybrid AC/DC LVDNs.

$$\begin{cases} F_{UL}=f_1=\min C_{invest} \\ F_{UL}=f_2=\min I_{VUF} \end{cases} \tag{11}$$

The annual investments of the hybrid AC/DC LVDNs considering the DC conversion can be calculated as:

$$C_{invest}=\sum_{n=1}^{N_{VSC}}\lambda C_{VSC}S^n_{VSC} \tag{12}$$

$$\lambda = \frac{r(1+r)^l}{(1+r)^l - 1} \tag{13}$$

Minimizing the three-phase unbalanced degree of the hybrid AC/DC LVDNs is also the objective of the lower level, and a detailed calculation is described in the next subsection. In the process of solving this model, the lower-level results is returned to the upper level to calculate the overall objectives.

The installed capacity of each VSC should meet the maximum capacity constraint.

$$S_{VSC}^{n} \le S_{VSC}^{\max} \tag{14}$$

The VSC locations are determined by which line is converted to DC operation and the candidate interconnection locations between the converted DC line and other AC lines. Therefore, the connection locations of VSCs should meet the following constraint.

$$L_{VSC}^{n} \in L_{VSC} \tag{15}$$

B. Lower-level Optimization Model

At the lower level, the three-phase power of the interconnection VSCs is optimized to minimize the three-phase unbalanced degree. The unbalanced degree of the LVDNs is expressed as the sum of the voltage unbalanced factors (VUFs) of all nodes, where the VUF of node *i* can be calculated according to the three-phase average voltage of the node [29], [30], as shown in (16) and (17).

$$F_{LL} = I_{VUF} = \sum_{t=1}^{T} \sum_{i \in N_{AC}} I_{VUF,i} \tag{16}$$

$$\begin{cases} I_{VUF,i} = \max(|V_i^{\varphi} - V_i^{avr}|/V_i^{avr}) \times 100\% \\ V_i^{avr} = (V_i^a + V_i^b + V_i^c)/3 \end{cases} \tag{17}$$

Power flow constraints of the hybrid AC/DC LVDN are considered in the lower-level optimization.

$$\begin{cases} \sum_{k \in \Psi_i} P_{ik}^{\varphi} = \sum_{j \in \Phi_i} (P_{ji}^{\varphi} - R_{ji}^{\varphi} (I_{ji}^{\varphi})^2) + P_i^{\varphi} \\ \sum_{k \in \Psi_i} Q_{ik}^{\varphi} = \sum_{j \in \Phi_i} (Q_{ji}^{\varphi} - X_{ji}^{\varphi} (I_{ji}^{\varphi})^2) + Q_i^{\varphi} \\ (V_i^{\varphi})^2 = (V_j^{\varphi})^2 - 2(R_{ji}^{\varphi} P_{ij}^{\varphi} + X_{ji}^{\varphi} Q_{ij}^{\varphi}) + ((R_{ji}^{\varphi})^2 + (X_{ji}^{\varphi})^2)(I_{ji}^{\varphi})^2 \\ (I_{ji}^{\varphi})^2 (V_j^{\varphi})^2 = (P_{ij}^{\varphi})^2 + (Q_{ij}^{\varphi})^2 \end{cases} \quad \forall i,j \in N_{AC} \tag{18}$$

$$\begin{cases} \sum_{k \in \Psi_i} P_{ik} = \sum_{j \in \Phi_i} (P_{ji} - R_{ij} I_{ji}^2) + P_i \\ V_i = V_j - I_{ji} R_{ij} \end{cases} \quad \forall i,j \in N_{DC} \tag{19}$$

It should be noted that (19) is the power flow equation for one DC circuit and the equation of each DC circuit in the selected DC structure needs to be considered. There are two DC circuits in the DC conversion structure of the urban and town LVDNs, and three circuits of the rural LVDNs.

The active power regulation of the VSCs needs to satisfy the power balance constraint, in which the converter losses are considered.

$$\left| P_{VSC}^{AC} \right| = \left| P_{VSC}^{DC} \right| + P_{VSC}^{loss} \tag{20}$$

Please note that the absolute value of the active power is used in (20), wherein if $P_{VSC}^{loss} > 0$, the active power of VSC flows from the AC to DC network.

Generally, the power losses of VSCs are about 2% [31]. Therefore, P_{VSC}^{loss} is calculated as:

$$P_{VSC}^{loss} = 0.02 P_{VSC}^{rate} \tag{21}$$

The following inequality constraints are also considered, including voltage constraints, line transfer capacity constraints and VSC capacity constraints.

$$V_{\min} \le V_i \le V_{\max} \tag{22}$$

$$P_{ji} \le P_{\max}^{DC} \quad \forall i,j \in N_{DC} \tag{23}$$

$$S_{ji}^{AC} \le S_{\max}^{AC} \quad \forall i,j \in N_{AC} \tag{24}$$

$$\sqrt{(P_{VSC}^{AC})^2 + (Q_{VSC}^{AC})^2} \le S_{VSC}^{n} \tag{25}$$

It should be noted that the maximum power transfer capacity of DC line is related to the converter configuration, which can be calculated by (8)-(10).

The optimization results of the lower-level model, including the three-phase power outputs of the VSCs and three-phase unbalanced degree, will be used to update the objectives and generate a better result for the hybrid AC/DC LVDNs.

The proposed optimal planning method only consider the external features of the VSC, i. e., the active and reactive power outputs of the VSC. The proposed optimal planning method can be applied to the configuration of various types of converters. It is needed to modify the unit capacity cost and power loss coefficient according to the converter type.

C. Algorithm of Proposed Optimization Model

The power outputs of VSCs are optimized at the lower level, which is an optimal power flow problem of the hybrid AC/DC LVDN. The second-order cone relaxation method and CPLEX solver are used at the lower level. The optimality and convergence of the optimal power flow (OPF) based on the second-order cone programming model have been proven in [32].

Based on [32], power flow constraint of the LVDNs (18) and VSC capacity constraint (25) can be converted to a second-order cone programming (SOCP) model. The constraints are converted to constraints (26) and (27).

$$\begin{cases} \sum_{k \in \Psi_i} P_{ik}^{\varphi} = \sum_{j \in \Phi_i} (P_{ji}^{\varphi} - R_{ji}^{\varphi} I_{2ji}^{\varphi}) + P_i^{\varphi} \\ \sum_{k \in \Psi_i} Q_{ik}^{\varphi} = \sum_{j \in \Phi_i} (Q_{ji}^{\varphi} - X_{ji}^{\varphi} I_{2ji}^{\varphi}) + Q_i^{\varphi} \\ V_{2i}^{\varphi} = V_{2j}^{\varphi} - 2(R_{ji}^{\varphi} P_{ij}^{\varphi} + X_{ji}^{\varphi} Q_{ij}^{\varphi}) + ((R_{ji}^{\varphi})^2 + (X_{ji}^{\varphi})^2) I_{2ji}^{\varphi} \\ (P_{ij}^{\varphi})^2 + (Q_{ij}^{\varphi})^2 \le I_{2ji}^{\varphi} V_{2j}^{\varphi} \end{cases} \quad \forall i,j \in N_{AC} \tag{26}$$

$$(P_{VSC}^{AC})^2 + (Q_{VSC}^{AC})^2 \le 2 \frac{S_{VSC}^{n}}{\sqrt{2}} \frac{S_{VSC}^{n}}{\sqrt{2}} \tag{27}$$

Consequently, the lower-level optimization model is transformed into the following SOCP problem.

$$\begin{cases} \min F_{LL} \\ \text{s.t. (16), (17), (19)-(24), (26), (27)} \end{cases} \tag{28}$$

As the upper-level optimization is a multi-objective problem with discrete variables, the upper-level model is solved

utilizing the non-dominated sorting genetic algorithm II (NSGA-II) [33]. The algorithm convergence can be improved by the GA with the elitist strategy and avoid suboptimal solutions. Moreover, the optimality is guaranteed by solving the model multiple times and adopting the optimal solution. The installed capacity of each location is encoded using a 3-bit binary number. In this encoding, "000" represents that the location does not have a VSC installed, and "001" represents the installation of a 20 kVA VSC.

The flowchart of the proposed optimal planning method is shown in Fig. 6. The initial population including locations and capacities of the VSCs is randomly generated at the upper level. Then, based on each scheme generated by the upper level, the lower-level optimization model is solved through CPLEX solver. The results of the lower level, including the three-phase power of the VSCs for 24 hours and three-phase unbalanced degree, are returned to the upper level. The objective function of the upper level is calculated and the population is updated. The iterations between the two levels are conducted to calculate the optimal configuration results. If the convergence condition or the maximum iteration of the upper level is satisfied, the calculation ends and the optimal planning results are obtained.

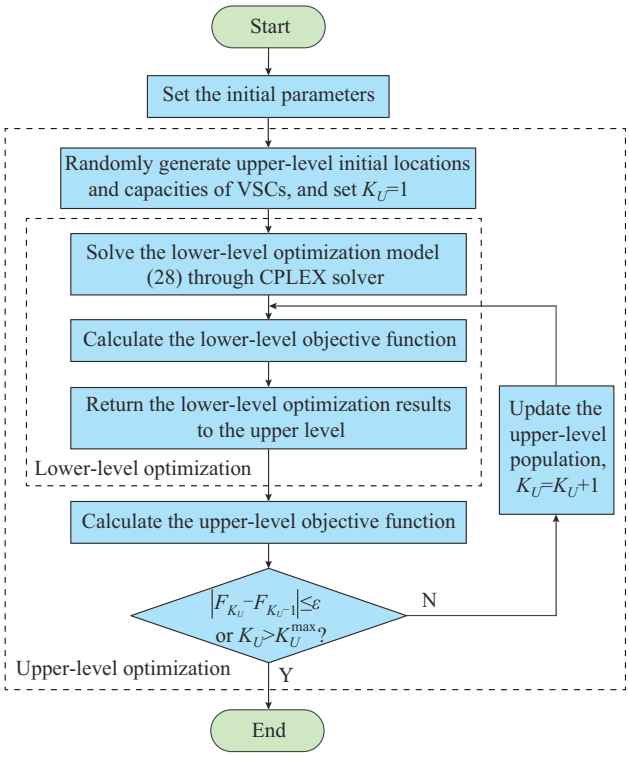

Fig. 6. Flowchart of proposed optimal planning method.

V. Simulation and Analysis

A. Simulation Background

The LVDN with integration of PVs and EVs shown in Fig. 1(a) is utilized to verify the proposed optimal planning method. In the case studies, LGJ-50 conductors with a maximum transfer capacity of 130 kW are used in the AC LVDN, while the transformers have a capacity of 500 kVA. The rated power of PV generation is 6 kW, the rated charging power of AC charging point is 7 kW, and that of DC charging point is 40 kW. Power curves of PV generations and loads are shown in Fig. 7. The capital cost of VSC is about 170 $/kVA [34]. The service life of VSC and the discount rate are set to be 15 years and 10%, respectively. The investments of VSCs connecting AC loads to DC lines are considered in (11), and the capacities of the VSCs are the maximum load in each node. The convergence accuracy and maximum iteration of NSGA-II are set to be 0.01 and 100, respectively.

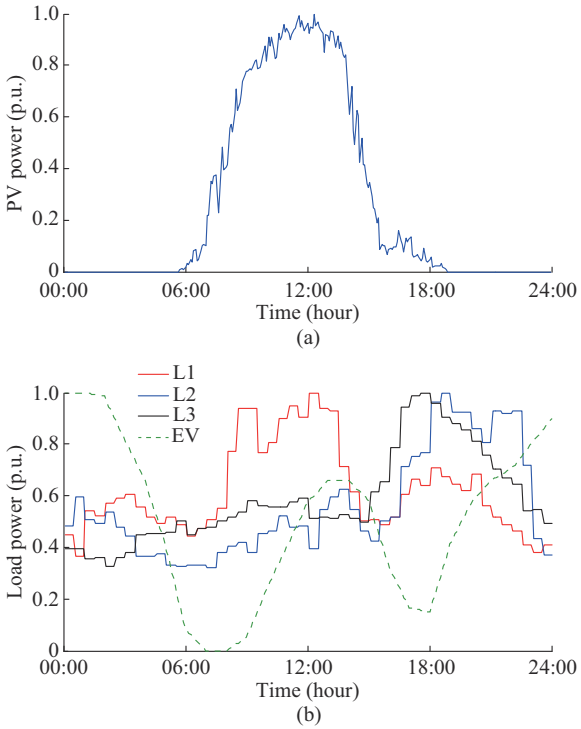

Fig. 7. Power curves of PV generations and loads. (a) PV power. (b) Load power.

B. Study 1: Superiority of Proposed Optimal Planning Method of Hybrid AC/DC LVDNs

The following five cases are designed and compared to verify the superiority of the proposed optimal planning method of the hybrid AC/DC LVDNs.

Case 1: AC LVDN.

Case 2: building new AC distribution lines.

Case 3: configuring SVGs in AC LVDN.

Case 4: configuring PCSs in AC LVDN.

Case 5: proposed optimal planning method of hybrid AC/DC LVDNs.

Case 1 is the base case without any configuration. To ensure a fair comparison, the configuration results of Cases 2-5 are obtained by solving the optimal planning model with the same objectives, i. e., the minimum annual investments and three-phase unbalanced degree. Moreover, the optimal operation is also considered in the planning process through the bi-level model. For the case of building new AC distribution lines, power flow calculation is conducted in the lower-level model, because there is no device to be dispatched. For

the cases of configuring SVGs and PCSs, the optimal dispatchings of the SVG and PCS are separately considered in their optimal planning models, in which the optimal dispatching strategy in [7] is adopted.

The maximum load level and PV accommodation capacity of LVDN are mainly determined by voltage limits and line transfer power limits. Under the assumption that load demand gradually increases, the AC network reaches its maximum load level at 325 kW, when the lowest voltage drops to 0.93 p.u.. The maximum PV accommodation capability of the AC network is about 117% of the system rated load, when the highest voltage reaches 1.07 p.u..

The five cases are compared from the following three aspects: the maximum load and PV capabilities, economic indices, voltage deviation and voltage unbalance.

1) Comparison of Maximum Load and PV Capabilities

Configuration results of Cases 2-5 are illustrated in Fig. 8. In addition, the comparison of the maximum load level and PV accomodation rate under different cases is illustrated in Table I.

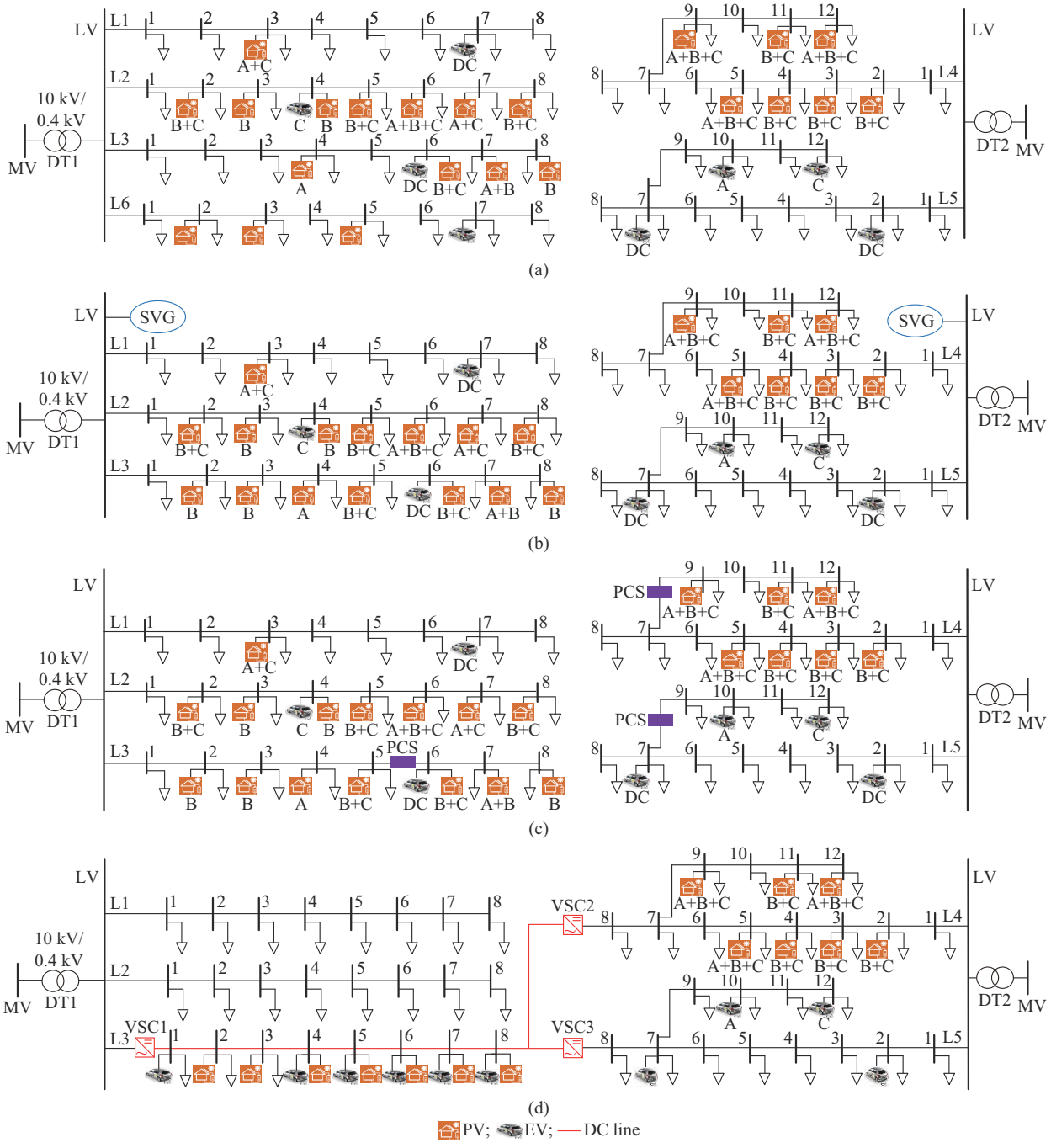

Fig. 8. Configuration results of Cases 2-5. (a) Case 2. (b) Case 3. (c) Case 4. (d) Case 5.

In Case 2, to eliminate the voltage violations of the AC LVDN, a new LV line is built (marked as L6), as shown in Fig. 8(a). Meanwhile, some of the loads and PVs of the L4 and L5 can be moved to the new-built line. The maximum

load level and maximum PV accomodation rate in Case 2 are increased to 410 kW and 145% compared with those of Case 1, respectively.

In Case 3, two SVGs with capacities of 30 kvar and 50 kvar are configured at the terminal of DT1 and DT2, as shown in Fig. 8(b). In Case 4, the three PCSs are configured in L3, L4, and L5, because the unbalanced issues mainly occur in these three lines, as illustrated in Fig. 8(c). The maximum load or PV accommodation rate in Case 3 and Case 4 is less increased compared with base case shown in Table I. This is because the configuration of SVGs and PCSs can alleviate voltage violations and unbalanced problems, thereby increasing the load and PV capacities. However, the transfer capacities of LVDN have not been fundamentally increased in Case 3 and Case 4.

TABLE I
COMPARISON OF THE MAXIMUM LOAD LEVEL AND PV ACCOMODATION RATE

Case	The maximum load level (kW)	The maximum PV accommodation rate (%)
1	325	117
2	410	145
3	350	125
4	340	120
5	546	210

In Case 5, the converted DC line L3 is interconnected with L4 and L5 by VSC2 and VSC3, as illustrated in Fig. 8(d). The benefits of the hybrid AC/DC LVDN in this case can be fully utilized because the power demands of L4 and L5 are complementary. Moreover, coordinated power control between L3-L5 is also achieved through optimal dispatching during configuration. The bipolar configuration with a dedicated metallic return shown in Fig. 3(e) is selected in this case, and the capacities of the VSCs are 100 kVA. The maximum PV accommodation rate is increased to 210%, and the maximum load level is increased to 546 kW in Case 5.

2) Comparison of Economic Indices

The cost of the configuration schemes is the investment of the installed devices. The annual profits of the configuration schemes include the power loss reduction $C_{save,loss}$ and the increase of PV accommodation $C_{save,PV}$. Therefore, the payback time Y_{PBT} can be calculated in terms of the cost and the annual profit. The economic indices in different cases at the current load level are shown in Table II.

TABLE II
ECONOMIC INDICES IN DIFFERENT CASES

Case	C_{invest} ($)	$C_{save,PV}$ ($)	$C_{save,loss}$ ($)	Y_{PBT} (year)
2	17000	1413	1042	6.92
3	10880	404	428	13.07
4	1020	151	149	3.39
5	56103	4692	1547	8.99

Configuring PCSs needs the lowest investment and lowest profit, and the payback time is only 3.39 years, which is the most economical scheme. The investment of configuring SVGs is lower than building new AC lines and hybrid AC/DC LVDN, but the payback time is the longest. Building new AC lines can effectively increase the PV integration and reduce power losses, and the payback time is 6.92 years. The hybrid AC/DC LVDN has the highest investment and profit, and the investment can be returned in 8.99 years. With the growth of load and the further increase of PV integration, the payback time will be further reduced.

3) Comparison of Voltage Deviation and Voltage Unbalance

The maximum voltage deviation and VUF under different cases are shown in Fig. 9(a) and Fig. 9(b), respectively. The VUF index of all 48 nodes during 24 hours is sorted from the highest to lowest, and then the statistical characteristics of VUF can be obtained, as shown in Fig 9(b).

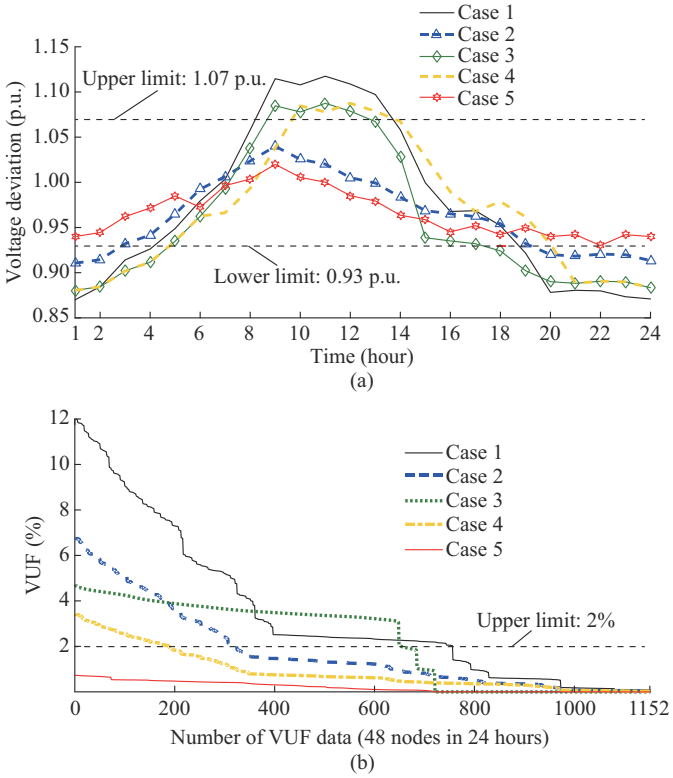

Fig. 9. Voltage profiles under different cases. (a) The maximum voltage deviation. (b) VUF.

In Case 1, over-voltage issues occur at midday and under-voltage issues occur at night, which are caused by the high PV output at midday and high EV charging load at night. Meanwhile, more than 65% of the sampling data of the VUF are larger than 2% in Case 1, and the maximum VUF is 12%.

Voltage violations and unbalanced issues still happen in Case 2 with a newly built AC line. This is because the new line is not interconnected with DT2, and the improvement of power quality is limited to the area of DT1 station.

Configuring SVGs and PCSs can effectively alleviate the unbalanced problem. The maximum VUF decreases to 4.5% and 3.3% in Case 3 and Case 4, respectively. However, the voltage violation problem has not been completely eliminated.

Power quality issues in hybrid AC/DC LVDN are com-

pletely eliminated. Voltage violations are eliminated by power coordination between the interconnected lines. Moreover, the three-phase power control of VSCs helps to improve the unbalanced issues and the maximum VUF is 0.73%.

Figure 10 shows the comparison of the different cases. The maximum PV accommodation rate and load level of the hybrid AC/DC LVDN are increased to 1.79 times and 1.68 times of those of the AC LVDN, respectively. The VUF index is reduced to 0, which means the unbalanced issues are completely eliminated. That is because the optimal power flow between lines and phases is achieved by power regulation of VSCs.

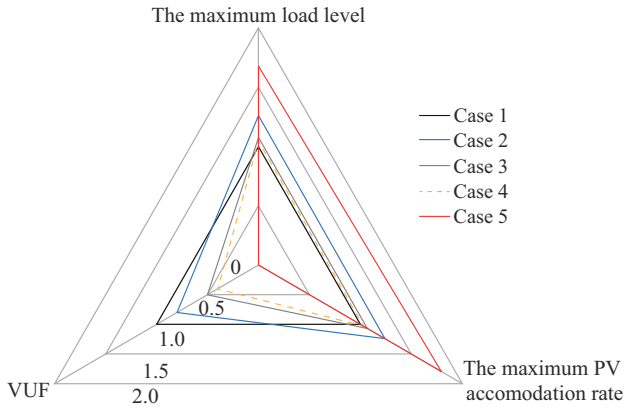

Fig. 10. Comparison of different cases.

C. Study 2: Feasibility of Hybrid AC/DC LVDNs

Assuming that the LVDN is fully loaded with the increase of the load, the LVDN can only be expanded or converted, and the configurations of SVGs and PCSs are no longer applicable. In order to verify the feasibility of the proposed optimal planning method, two schemes of hybrid AC/DC LVDN and building new AC lines are comparatively analyzed, considering the total amount of new loads and the proportion of DC loads in new loads. The investment situations with different load ratio are shown in Fig. 11.

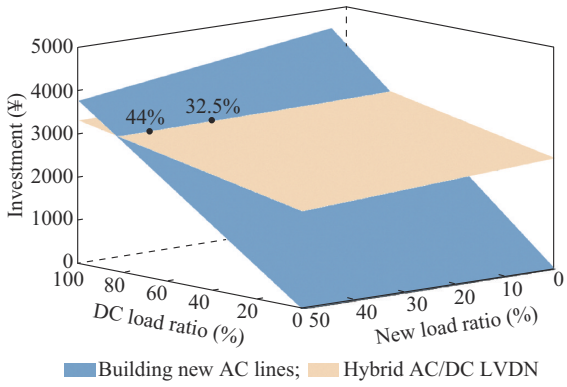

Fig. 11. Investment situations with different load ratio.

The following conclusions can be drawn from Fig. 11. When the ratio of the new load to the original load is in interval 1 ([0%, 32.5%]), building new AC lines is the better scheme with lower investment. This shows that the cost of converter station is dominant in all the factors that affect the investment in this interval.

When the ratio of the new load is in interval 2 ([32.5%, 44%]), the optimal scheme is mainly affected by the proportion of DC load. In this interval, as the amount of new load increases, the minimum threshold of the DC load ratio that determines the economics of the hybrid AC/DC LVDN is reduced from 100% to 0%. This is because that the investment of converter related to the DC load is the main factor affecting the investment in this interval.

When the ratio of the new load is in interval 3 ([44%, 50%]), hybrid AC/DC LVDN is the better scheme. This result shows that, in this interval, the investment related to the new-built AC lines dominates all the factors that affect the investment in this interval.

With the development of DC technologies, the cost of converter stations would be gradually reduced. However, the cost of building new lines will be more expensive, due to the limited land in urban areas. Based on the above reasons, the economic advantages of the DC conversion scheme will be more prominent in the future.

D. Analysis of a Real Distribution System

A large-scale LV system modified by a real system in Anhui Province, China, as shown in Fig. 12(a), is used to verify the effectiveness and scalability of the proposed optimal planning method. The configuration results of the proposed optimal planning method are shown in Fig. 12(b) and Table III.

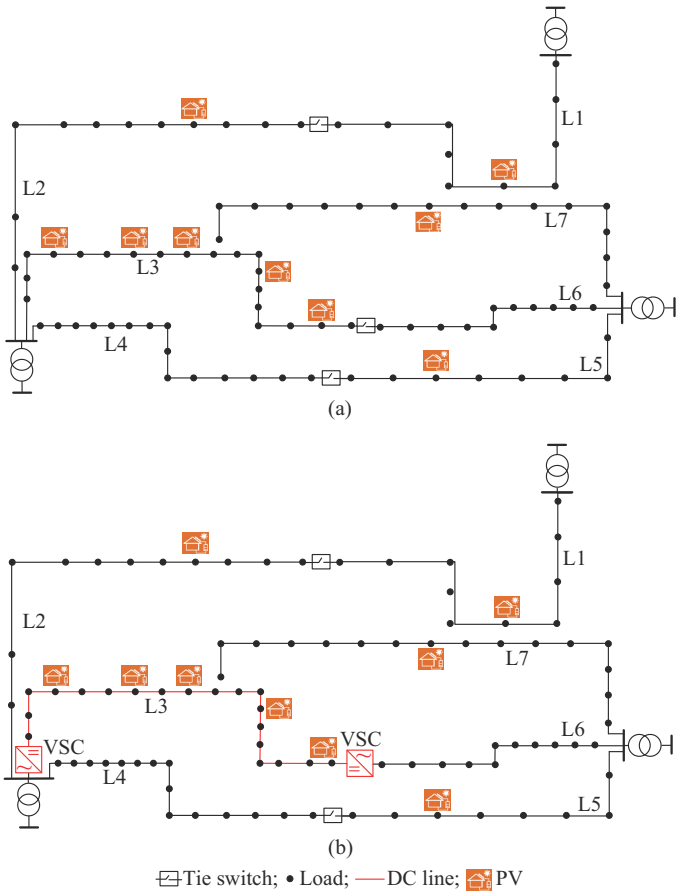

Fig. 12. Configuration of hybrid AC/DC LVDN. (a) A modified real system. (b) Configuration result.

TABLE III
ECONOMIC INDICES OF CONFIGURATION

Economic index	Value
Total investment ($)	67154.00
Annual Power losses reduction ($)	1687.00
Annual increase of PV accommodation ($)	5066.00
Payback time (year)	9.94

In this case, L3 is converted to DC and interconnected with L6 by VSC, and coordinated power control between two lines is also achieved through optimal dispatching of VSCs. The maximum PV accommodation rate is increased by 7.25%, because of the large power transfer capacity and LV drop of DC operation and flexible power transfer between L3 and L6. The maximum load level is also increased by 25.5% because load power and PV outputs are complementary between the two lines. The economic indices of this configuration are shown in Table III, and the payback time is 9.94 years.

The simulation program of this paper is conducted on the MATLAB R2016a-YALMIP platform, utilizing the CPLEX solver. The hardware device used for the simulation is a computer with a 2.2 GHz Intel Core i5-5200 processor and 12 GB of RAM. The computation time is about 20 min for the five-line system in Section V-B, and 23 min for the real system in this subsection.

VI. CONCLUSION

An optimal planning method of hybrid AC/DC LVDNs considering the DC conversion from AC lines is proposed. DC configurations for three typical LVDNs in urban areas, town areas, and rural areas are analyzed. A bi-level optimal configuration model for hybrid AC/DC LVDNs is further proposed based on the selected DC configuration.

With the proposed optimal planning method considering DC conversion, the maximum PV accommodation rate and load level in the hybrid AC/DC LVDN are increased to 1.79 times and 1.68 times of the conventional AC LVDN, respectively. At the same time, the unbalanced issues are completely eliminated by power regulation of VSCs. The investment of the hybrid AC/DC LVDN can be returned in 9 years. With the growth of loads and the increase of PV integration, the payback time will be further reduced.

Simulation results show that in case the ratio of the new load is higher than 32.5%, the investment of the DC conversion is sensitive to the DC load ratio. If the ratio of the new load is higher than 44%, DC conversion is always the optimal investment scheme.

The optimal planning of hybrid AC/DC LVDNs considering the uncertainty of PVs can be further studied in the future.

REFERENCES

[1] X. Su, M. A. S. Masoum, and P. J. Wolfs, "Multi-objective hierarchical control of unbalanced distribution networks to accommodate more renewable connections in the smart grid era," *IEEE Transactions on Power Systems*, vol. 31, no. 5, pp. 3924-3936, Sept. 2016.

[2] M. Safayatullah, M. T. Elrais, S. Ghosh *et al.*, "A comprehensive review of power converter topologies and control methods for electric vehicle fast charging applications," *IEEE Access*, vol. 10, pp. 40753-40793, Oct. 2022.

[3] T. Chen, X. P. Zhang, J. Wang *et al*., "A review on electric vehicle charging infrastructure development in the UK," *Journal of Modern Power Systems and Clean Energy*, vol. 8, no. 2, pp. 193-205, Mar. 2020.

[4] P. Mohammadi and S. Mehraeen, "Challenges of PV integration in low-voltage secondary networks," *IEEE Transactions on Power Delivery*, vol. 32, no. 1, pp. 525-535, Feb. 2017.

[5] D. Sciano, A. Raza, R. Salcedo *et al*., "Evaluation of DC links on dense-load urban distribution networks," *IEEE Transactions on Power Delivery*, vol. 31, no. 3, pp. 1317-1326, Jun. 2016.

[6] M. Brenna, E. de Berardinis, L. D. Carpini *et al.*, "Automatic distributed voltage control algorithm in smart grids applications," *IEEE Transactions on Smart Grid*, vol. 4, no. 2, pp. 877-885, Jun. 2013.

[7] B. Liu, K. Meng, Z. Y. Dong *et al.*, "Unbalance mitigation via phase-switching device and static var compensator in low-voltage distribution network," *IEEE Transactions on Power Systems*, vol. 35, no. 6, pp. 4856-4869, Nov. 2020.

[8] R. You and X. Lu, "Voltage unbalance compensation in distribution feeders using soft open points," *Journal of Modern Power Systems and Clean Energy*, vol. 10, no. 4, pp. 1000-1008, Jul. 2022.

[9] D. Wu, F. Tang, T. Dragicevic *et al.*, "A control architecture to coordinate renewable energy sources and energy storage systems in islanded microgrids," *IEEE Transactions on Smart Grid*, vol. 6, no. 3, pp. 1156-1166, May 2015.

[10] K. Ma, W. Chen, M. Liserre *et al.*, "Power controllability of a three-phase converter with an unbalanced AC source," *IEEE Transactions on Power Electronics*, vol. 30, no. 3, pp. 1591-1604, Mar. 2015.

[11] A. Sannino, G. Postiglione, and M. H. J. Bollen, "Feasibility of a DC network for commercial facilities," *IEEE Transactions on Industry Applications*, vol. 39, no. 5, pp. 1499-1507, Sept. 2003.

[12] Z. Lin, X. Ruan, L. Jia *et al.*, "Optimized design of the neutral inductor and filter inductors in three-phase four-wire inverter with split DC-link capacitors," *IEEE Transactions on Power Electronics*, vol. 34, no. 1, pp. 247-262, Jan. 2019.

[13] F. Koyanagi and Y. Uriu, "A strategy of load leveling by charging and discharging time control of electric vehicles," *IEEE Transactions on Power Systems*, vol. 13, no. 3, pp. 1179-1184, Aug. 1998.

[14] G. Abeynayake, G. Li, T. Joseph *et al.*, "Reliability and cost-oriented analysis, comparison and selection of multi-level MVDC converters," *IEEE Transactions on Power Delivery*, vol. 36, no. 6, pp. 3945-3955, Dec. 2021.

[15] S. K. Chaudhary, J. M. Guerrero, and R. Teodorescu, "Enhancing the capacity of the AC distribution system using DC interlinks – a step toward future DC grid," *IEEE Transactions on Smart Grid*, vol. 6, no. 4, pp. 1722-1729, Jul. 2015.

[16] M. de Prada, L. Igualada, C. Corchero *et al.*, "Hybrid AC-DC offshore wind power plant topology: optimal design," *IEEE Transactions on Power Systems*, vol. 30, no. 4, pp. 1868-1876, Jul. 2015.

[17] U. Straumann and C. M. Franck, "Ion-flow field calculations of AC/DC hybrid transmission lines," *IEEE Transactions on Power Delivery*, vol. 28, no. 1, pp. 294-302, Jan. 2013.

[18] H. M. A. Ahmed, A. B. Eltantawy, and M. M. A. Salama, "A planning approach for the network configuration of AC-DC hybrid distribution systems," *IEEE Transactions on Smart Grid*, vol. 9, no. 3, pp. 2203-2213, May 2018.

[19] J. Yu, K. Smith, M. Urizarbarrena *et al.*, "Initial designs for the ANGLE DC project; converting existing AC cable and overhead line into DC operation," in *Proceedings of 13th IET International Conference on AC and DC Power Transmission (ACDC 2017)*, Manchester, UK, Jun. 2017, pp. 1-6.

[20] A. A. Eajal, M. F. Shaaban, K. Ponnambalam *et al.*, "Stochastic centralized dispatch scheme for AC/DC hybrid smart distribution systems," *IEEE Transactions on Sustainable Energy*, vol. 7, no. 3, pp. 1046-1059, Jul. 2016.

[21] X. Liu, P. Wang, and P. C. Loh, "A hybrid AC/DC microgrid and its coordination control," *IEEE Transactions on Smart Grid*, vol. 2, no. 2, pp. 278-286, Jan. 2011.

[22] L. Zhang, J. Liang, W. Tang *et al.*, "Converting AC distribution lines to DC to increase transfer capacities and DG penetration," *IEEE Transactions on Smart Grid*, vol. 10, no. 2, pp. 1477-1487, Mar. 2019.

[23] A. Ghadiri, M. R. Haghifam, and S. M. M. Larimi, "Comprehensive approach for hybrid AC/DC distribution network planning using genetic algorithm," *IET Generation, Transmission & Distribution*, vol. 11,

pp. 3892-3902, Jan. 2017.
[24] X. Liu, Y. Liu, J. Liu *et al.*, "Optimal planning of AC-DC hybrid transmission and distributed energy resource system: review and prospects," *CSEE Journal of Power and Energy Systems*, vol. 5, no. 3, pp. 409-422, Sept. 2019.
[25] A. Shekhar, L. M. Ramirez-Elizondo, T. B. Soeiro *et al.*, "Boundaries of operation for refurbished parallel AC-DC reconfigurable links in distribution grids," *IEEE Transactions on Power Delivery*, vol. 35, no. 2, pp. 549-559, Apr. 2020.
[26] A. Shekhar, E. Kontos, L. Ramirez-Elizondo *et al.*, "AC distribution grid reconfiguration using flexible DC link architecture for increasing power delivery capacity during (n–1) contingency," in *Proceedings of 2017 IEEE Southern Power Electronics Conference (SPEC)*, Puerto Varas, Jul. 2017, pp. 1-6.
[27] L. Zhang, Y. Chen, C. Shen *et al.*, "Optimal configuration of hybrid AC/DC urban distribution networks for high penetration renewable energy," *IET Generation, Transmission & Distribution*, vol. 12, no. 20, pp. 4499-4506, Oct. 2018.
[28] B. Kruizinga, P. A. A. F. Wouters, and E. F. Steennis, "High frequency modeling of a shielded four-core low voltage underground power cable," *IEEE Transactions on Dielectrics and Electrical Insulation*, vol. 22, no. 2, pp. 649-656, Apr. 2015.
[29] P. Wang, D. H. Liang, J. Yi *et al.*, "Integrating electrical energy storage into coordinated voltage control schemes for distribution networks," *IEEE Transactions on Smart Grid*, vol. 5, no. 2, pp. 1018-1032, Mar. 2014.
[30] W. Tang, Y. Cai, L. Zhang *et al.*, "Hierarchical coordination strategy for three-phase MV and LV distribution networks with high-penetration residential PV units," *IET Renewable Power Generation*, vol. 14, no. 19, pp. 3996-4006, Dec. 2020.
[31] W. Cao, J. Wu, N. Jenkins *et al*., "Benefits analysis of soft open points for electrical distribution network operation," *Applied Energy*, vol. 165, pp. 36-47, Mar. 2016.
[32] Q. Li, R. Ayyanar, and V. Vittal, "Convex optimization for DES planning and operation in radial distribution systems with high penetration of photovoltaic resources," *IEEE Transactions on Sustainable Energy*, vol. 7, no. 3, pp. 985-995, Jul. 2016.
[33] J. C. F. Caballero, F. J. Martinez, C. Hervas *et al.*, "Sensitivity versus accuracy in multiclass problems using memetic pareto evolutionary neural networks," *IEEE Transactions on Neural Networks*, vol. 21, no. 5, pp. 750-770, May 2010.
[34] Z. Wu, Q. Sun, W. Gu *et al.*, "AC/DC hybrid distribution system expansion planning under long-term uncertainty considering flexible investment," *IEEE Access*, vol. 8, pp. 94956-94967, Apr. 2020.

Bo Zhang received the B.S. degree in electrical engineering from China Agricultural University, Beijing, China, in 2016, where she is currently working toward the Ph. D. degree in agricultural electrification and automation with the College of Information and Electrical Engineering. Her main research interests include hybrid AC/DC distribution network, renewable energy generation, and economic operation of active distribution network.

Lu Zhang received the B.S. degree in electrical engineering and the Ph.D. degree in agricultural electrification and automation from China Agricultural University, Beijing, China, in 2011 and 2016, respectively. He was a postdoc in the Department of Electrical Engineering at Tsinghua University, Beijing, China, From 2017 to 2019. He is currently an Associate Professor at College of Information and Electrical Engineering, China Agricultural University. His main research interests include hybrid AC/DC distribution network, renewable energy generation, and active distribution networks.

Wei Tang received the B.S. degree in electrical engineering from Huazhong University of Science and Technology, Wuhan, China, in 1992, and the Ph.D. degree in electrical engineering from Harbin Institute of Technology, Harbin, China, in 1998. From 1998 to 2000, she was a post-doctor with Harbin Engineering University, Harbin, China. She is currently a Professor at the College of Information and Electrical Engineering, China Agricultural University, Beijing, China. Her research interests include economic and security operation of distribution network, distributed generation and active distribution network.

Gen Li received the B.Eng. degree in electrical engineering from Northeast Electric Power University, Jilin, China, in 2011, the M.Sc. degree in power engineering from Nanyang Technological University, Singapore, in 2013, and the Ph.D. degree in electrical engineering from Cardiff University, Cardiff, U.K., in 2018. He is now an Associate Professor in power system at the Technical University of Denmark (DTU), Ballerup, Denmark. From 2013 to 2016, he has been a Marie Curie Early Stage Research Fellow funded by the European Commission's MEDOW project. He has been a Visiting Researcher at China Electric Power Research Institute and Global Energy Interconnection Research Institute, Beijing, China, at Elia, Brussels, Belgium and at Toshiba International (Europe), London, U.K.. He was a Research Associate at the School of Engineering, Cardiff University from 2018 to 2022. His research interests include control and protection of high-voltage and medium-voltage DC systems, offshore wind power, offshore energy islands, reliability modelling and evaluation of power electronics systems.

Chen Wang received the B.S. and M.S. degrees in electrical engineering from China Agricultural University, Beijing, China, in 2017 and 2021, respectively. He is currently with the State Grid Beijing Electric Power Research Institute, Beijing, China. His main research interests include hybrid AC/DC distribution network, renewable energy generation, and active distribution networks.